Comparability of FDG PET Studies in Probable Alzheimer's Disease

K. Herholz, D. Perani, E. Salmon, G. Franck, F. Fazio, W.-D. Heiss and D. Comar

Max-Planck-Institut für Neurologische Forschung, Cologne, Germany; Istituto di Technologie Biomediche Avanzate, Hospital San Raffaele, Medizina Nucleare, Milan, Italy; and Université de Liège, Centre de Recherches du Cyclotron, Liège, Belgium

Results of studies with positron emission tomography (PET) of ^{18}F-2-fluoro-2-deoxy-D-glucose (FDG) in patients with probable Alzheimer's disease (AD) were compared among three European centers with different PET scanners (in-plane resolution ranging between 6.75 mm and 9.2 mm). A ratio of glucose metabolism in the most typically affected regions over the least typically affected regions was calculated to quantitatively analyze the characteristic pattern of AD. Diagnostic accuracy of this composite ratio was high (95.8%) and was superior to that of most ratios derived from single regions. Correspondingly, there was a consistent, highly significant difference between patients (mean ratio 0.77 ± 0.11) and normals (mean 0.99 ± 0.04) without significant differences among laboratories. Possible small effects of rate constant variation and region size were analyzed by computer simulation. The results demonstrate that a common investigation protocol may yield FDG PET data in different laboratories that are closely comparable in spite of differences between scanners and imaging equipment.

J Nucl Med 1993; 34:1460–1466

Previous positron emission tomography (PET) studies with ^{18}F-2-fluoro-2-deoxy-D-glucose (FDG) have shown a characteristic pattern of metabolic impairment of cortical association areas in Alzheimer's disease (AD) (*1–6*). Impairment of glucose metabolism in temporoparietal and frontal areas is in contrast with relatively well preserved metabolism in primary visual and sensorimotor areas, basal ganglia and cerebellum. In early stages of the disease, the typical pattern may not yet be complete. In particular, frontal involvement may be missing and temporoparietal metabolism may only be unilaterally impaired. In spite of these limitations, it has been suggested that FDG PET may be used for early diagnosis of AD (*7*), which would be very valuable for therapeutic trials in early stages of the disease.

As yet, inclusion of PET in multicenter studies has been hampered by a lack of standardization in reporting results, making comparisons between different laboratories extremely difficult. Therefore, we analyzed whether a study protocol based on a robust ratio to assess the typical metabolic pattern of AD can yield comparable results in three different laboratories.

Received Aug. 20, 1992; revision accepted May 25, 1993.

For correspondence and reprints contact: Dr. Karl Herholz, Max-Planck-Institut für neurologische Forschung, Gleueler Str. 50, W-5000 Köln 41, Germany.

PATIENTS AND METHODS

Thirty-seven patients (21 men and 16 women, mean age 65.2 ± 7.4 yr) and 34 healthy control subjects (17 men and 17 women, mean age 57.1 ± 13.5 yr) were entered into the study at three centers located in Cologne, Germany, Milan, Italy and Liège, Belgium. Patient-entry criteria were the clinical diagnosis of probable AD according to the criteria of the NINCDS-ADRDA working group (*8*) and age limits between 40 and 80 yr. All patients underwent general medical, neurological and psychiatric examination by an experienced neurologist. Standard laboratory tests were performed to exclude hematological or systemic metabolic disorders. Focal brain lesions were excluded by CT or MRI. All patients underwent detailed neuropsychological testing including assessment of memory impairment and mini-mental status examination (MMSE) (*9*).

Distribution of age, sex and severity (MMSE) did not differ significantly among patient groups (see Table 3). Mean overall patient age was 65.2 ± 7.4 yr, indicating that patients with presenile and senile age of onset were approximately balanced. Only in patients from the center in Milan was the age distribution slightly skewed toward the presenile group (median age 59, mean 64.5 yr, $p = 0.052$ in the Shapiro-Wilk test of normality). Recruitment of normals was different among centers. Healthy normal volunteers were studied who were significantly younger than patients in the centers in Liège (58.2 ± 8.0 yr versus 65.8 ± 5.8 yr, $p = 0.025$) and Milan (44.6 ± 15.7 yr versus 64.5 ± 8.7 yr, $p = 0.001$). Ages of controls and patients were similar in the center in Cologne (65.4 ± 7.3 yr versus 65.6 ± 7.6 yr) but controls included individuals with subjective minor memory complaints who proved healthy in clinical examination and extensive neuropsychological testing (including MMSE of 28 or higher). Distribution of sexes was comparable between patients and normals in all centers.

PET scanning was performed under resting conditions with eyes closed and ears without plugs in a room with low background noise. Multiple slices parallel to the canthomeatal line from the cerebellum to a level at least 27 mm above the basal ganglia were acquired. Tomograms were reconstructed by filtered backprojection and corrected for attenuation. Metabolic rates of glucose (MRGlu) were calculated from measured activity in the brain and in multiple blood samples according to the FDG model (*10,11*). Details of methods used depended on intrinsic machine and software properties in each laboratory as summarized in Table 1. Rate

TABLE 1
Technical Details Differing Between Centers

	Center		
	Milan	Liège	Cologne
Scanner type	Ecat 931/04-12	NeuroEcat	Scanditronix PC-384
No. planes × no. bed positions	7 × 2	2 × 6	7 × 2
Slice thickness (mm)	6.75	14.2	11
In-plane resolution (FWHM, mm)	6.0	9.2	7.8
Attenuation correction method	Measured with ^{68}Ge ring source	Ellipse	Head contour
K_1 (ml/g/min)	0.105	0.102	0.0904
k_2 (min^{-1})	0.148	0.103	0.1377
k_3 (min^{-1})	0.074	0.062	0.0715
k_4 (min^{-1})	0.0	0.0058	0.0
FDG dose (MBq)	250–300	300	185
Start of scanning (min postinjection)	45	45	30
Region shape	Circles*	Ellipse	Sector
Average size (cm^2)	2.2	2.5	2.8
Blood samples	Radial artery	Radial artery	Arterialized dorsal hand vein†

*Regions consisted of 2 to 4 circles (Fig. 1), each 0.72 cm^2 resulting in an average region size of 2.2 cm^2.
†Arterialization by 44°C water bath, checked by blood gas analysis.

constants used had been determined in normals in the center in Cologne (*12*) or were taken from the literature in the centers in Milan (*13*) and Liège (*11*).

In each laboratory an experienced physician performed visual examination of metabolic images, reading them with a background of clinical information as done in daily clinical practice.

Location of regions of interest (ROIs) was defined with reference to the level best representing the basal ganglia. Brain convexity regions lay between two radial angles originating in the center of each slice and ranging in each hemisphere from 0° (frontal pole) to 180° (occipital pole). Generally, regions were shaped to sample gray matter and to exclude white matter as far as possible. Regional MRGlu was determined in regions typically most affected (A) and in regions typically least affected (N) by AD. Regions of Group A were located in the frontal association cortex and the temporoparietal association cortex. Typically, least affected regions (N) were located in the primary sensorimotor cortex, primary visual cortex, putamen and cerebellum. Details of region locations are listed in Table 2 and typical regions are shown in Figure 1. A composite metabolic ratio, previously developed by Herholz et al. (*14*), was calculated by averaging MRGlu over all specified regions from both hemispheres in each group, A and N, and then dividing the mean regional MRGlu of Group A through that of Group N.

For comparison of sensitivity and specificity of this composite ratio, 16 ratios of single regions were also calculated. Thus, MRGlu in left temporoparietal, right temporoparietal, left frontal or right frontal cortex was divided through MRGlu in primary sensorimotor cortex, primary visual cortex, putamen or cerebellum. MRGlu in the denominator regions was always averaged over both sides.

Statistical methods included analysis of variance (ANOVA) and analysis of covariance (ANCOVA) with Tukey's studentized range method for multiple means comparisons among groups and

TABLE 2
Region Localization

Anatomical location	Approximate axial level*	In-plane location
Group A		
Prefrontal cortex	+27 mm	Sector 20°–40°
Temporoparietal cortex	13 mm	Sector 120°–140°
Temporoparietal cortex	0 mm	Sector 120°–140°
Temporoparietal cortex	−13 mm	Sector 100°–120°
Group N		
Primary sensorimotor cortex	+27 mm	Sector 80°–100°
Primary visual cortex	Slice with most active representation	Most active pericalcarine area
Putamen	0 mm	
Cerebellum	Slice with best representation	Cerebellar cortex

*Relative to level that represents basal ganglia best.

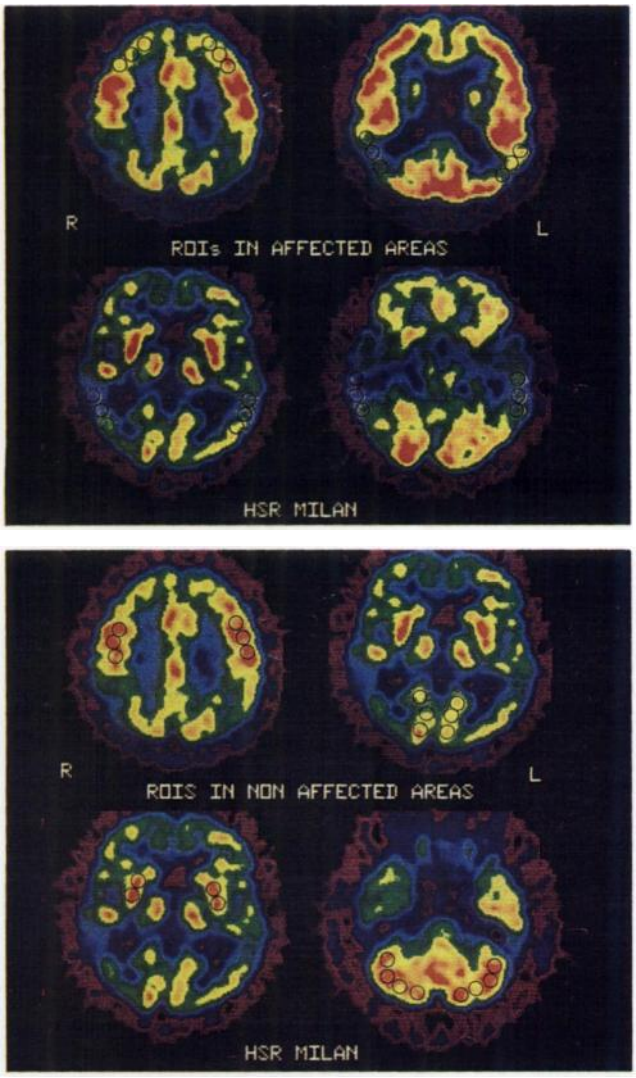

FIGURE 1. Metabolic maps of a 59-yr-old patient with early mild dementia of Alzheimer type showing the typical pattern. ROIs for calculation of the metabolic index according to the study protocol are demonstrated. Typically most affected areas (Group A, numerator) are shown in the upper part: frontal association cortex 27 mm above basal ganglia, temporoparietal cortex in three levels (13 mm above, at level of basal ganglia, and 13 mm below). Typically least affected areas (Group N, denominator) are shown in the lower part: primary sensorimotor cortex, primary visual cortex, putamen and cerebellum.

the chi-square test. Receiver operating characteristic (ROC) curves were calculated by variation of the threshold to compare the diagnostic accuracy of the composite with the other ratios and Wilcoxon statistics were used to assess significance (*15*). Data were distributed normally and values are reported as means ± s.d. All calculations were performed using the SAS software package (SAS Institute, Cary, NC).

Simulation Studies

To evaluate the influence of variation of rate constants and region size, the patient data of the center in Cologne underwent additional calculations. We studied the effect of increasing K_1 by 10%, decreasing k_2 or k_3 by 10% or increasing k_4 from 0.0 to 0.005 min^{-1}. In addition, the combinations of rate constants used in the centers in Milan and Liège were applied to the activity data recorded in the center in Cologne. Region size was varied by modification of the computerized mapping procedure (*16*) used in the center in Cologne.

RESULTS

Visual examination of metabolic maps confirmed a high frequency of the typical pattern (Fig. 1), i.e., bilateral temporoparietal hypometabolism and optional frontal hypometabolism, in contrast to relatively normal metabolism in primary visual and sensorimotor cortex, basal ganglia and cerebellum in most patients from all centers (Milan: 12 of 13; Liège: 10 of 10; and Cologne: 11 of 14). In some patients, pronounced right or left asymmetry was noted and three patients (one from the center in Milan; two from the center in Cologne) had unilateral temporoparietal hypometabolism only. Frontal predominance of hypometabolism was noted in one patient from the center in Liège.

Metabolic ratios in patients were significantly lower than in controls in all centers (Table 3) indicating that the ratio approach was appropriate to assess the metabolic pattern. Patient mean values were lowest in the center in Milan and highest in the center in Cologne, but differences were not significant ($p = 0.14$ in ANOVA).

Previous studies indicate that the metabolic ratio depends on patient age and dementia severity (*17*). To examine this influence and correct for it, an ANCOVA with age and MMSE as covariates was performed. As expected, a significant increase of the ratio with age was found ($p = 0.013$, Fig. 2). A tendency toward association of the ratio with MMSE scores was also present but not significant ($p = 0.07$). With adjustment for these two variables, there again was no significant difference of the ratio among the centers ($p = 0.72$).

In controls, no dependence of the ratio on age was found. As shown in Figure 3, the mean value was very

TABLE 3
Pertinent Data (mean ± s.d.) of Patients and Controls

Center	Group	No. (M/F)	Age (yr)	MMSE	Metabolic ratio
Milan	AD	9/4	64.5 ± 8.7	19.6 ± 3.3	0.72 ± 0.10
	Controls	5/5	44.6 ± 15.7	—	0.98 ± 0.03
Liège	AD	5/5	65.8 ± 5.8	20.7 ± 6.0	0.78 ± 0.11
	Controls	5/5	58.2 ± 8.0	—	1.02 ± 0.03
Cologne	AD	7/7	65.6 ± 7.6	20.1 ± 4.5	0.81 ± 0.11
	Controls	7/7	65.4 ± 7.3	—	0.98 ± 0.04

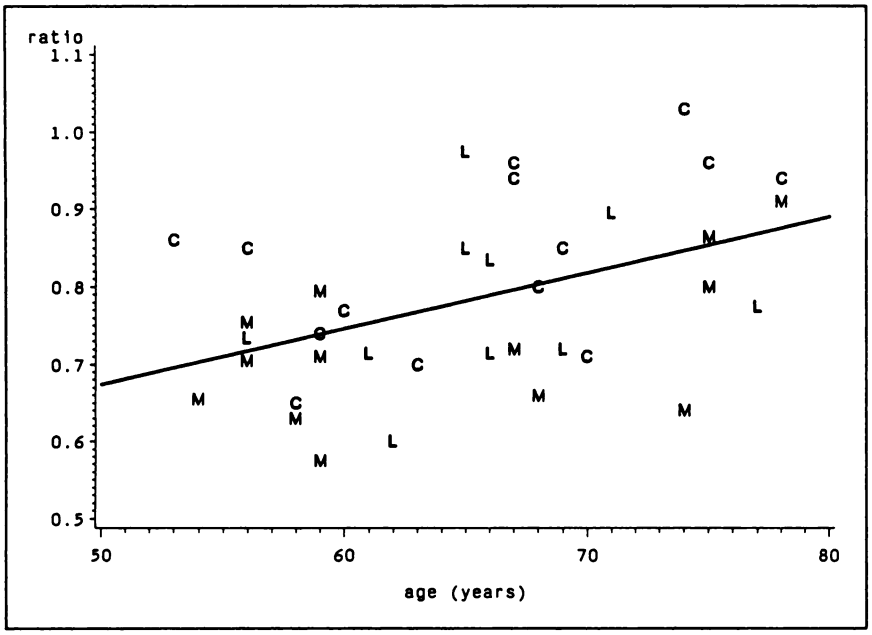

FIGURE 2. Scatter plot of metabolic ratio in patients and its significant dependency on age ($p = 0.013$) in the various centers, demonstrating that there was no significant difference of ratio values and their age-dependence between centers.

close to 1.0 over the entire age range. There was a tendency towards larger scattering in the older controls that was, however, not significant in an F-test.

The metabolic ratio, as a construct that represents the typical pattern of metabolic alterations in AD, yielded a better separation of patients from normals than ratios of single regions. As illustrated by ROC curves in Figure 4, 68 of the 71 subjects (95.8%) were classified correctly at a threshold of 0.921 for the metabolic ratio. Corresponding sensitivity (percentage of true positives) was 94.6% and specificity (percentage of true negatives) was 97.0%. The area under the ROC curve covered 97.8% (standard error 1.5%). Ratios derived from single regions yielded smaller areas under the ROC curve (Table 4) than the composite ratio and this was significant ($p < 0.05$) for all regions except the left temporoparietal cortex through the cerebellum, which came closest to the results of the composite ratio.

In the simulation studies, a 10% increase of K_1 decreased the ratio in patients on average by 1.12%. A decrease of the ratio of 0.8% was caused by a 10% decrease of k_2; a decrease of the ratio of 0.37% by a 10% decrease of k_3; and a decrease of the ratio of 0.84% by using a k_4 of 0.005 min^{-1} instead of 0.0. These changes were considerably smaller than those of regional metabolic rates (corresponding decreases of 4.3%, 2.4%, 1.1% and 4.5%, respectively). Decreases were more pronounced in regions with low metabolism, such as temporoparietal regions affected by the disease. Consequently, the effect of rate constant variation was stronger on lower ratios, whereas normal ratios close to one were barely affected. The combination of rate constants used in the center in Liège applied to the data of the center in Cologne resulted in a decrease of the ratio by 7.7%, whereas metabolic rates were reduced by 15.9% on average. The combination used in the center in Milan was more similar to the center in Cologne; it resulted in a 0.9% decrease of the ratio (4.2% for metabolic rates).

Region size also affected the ratio slightly; a 10% increase of region size increased the ratio by 1.2%. The magnitude of this effect was about the same as for regional metabolic rates, they declined on average by 1.0%. This decline occurred mainly in the relatively normal regions that composed the denominator (it was virtually absent in severely hypometabolic regions). Thus, dependency of the

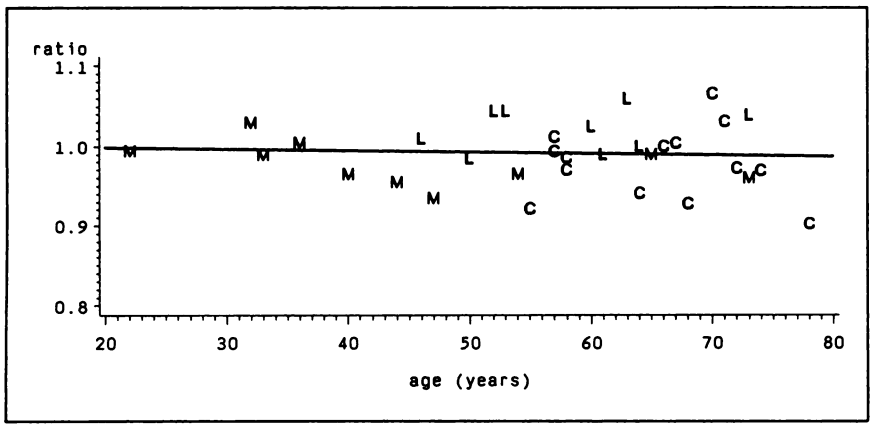

FIGURE 3. Scatter plot of metabolic ratio in controls (same arrangement as in Fig. 2), demonstrating that age-dependence or differences between centers did not exist.

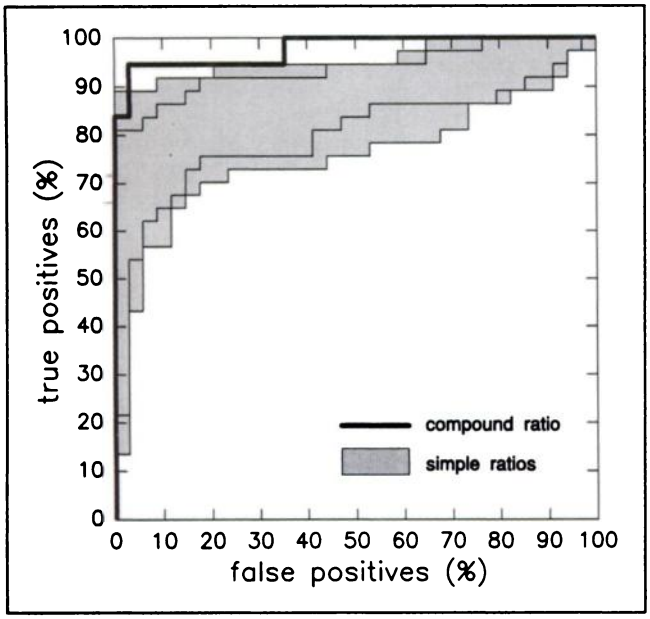

FIGURE 4. ROC curves of the diagnostic accuracy of the composite metabolic ratio (typically most affected through typically least affected regions, thick line) compared with ratios of single regions (shaded area). Among the latter, the relatively best accuracy was achieved by left or right temporoparietal cortex through cerebellum, the least accuracy by left or right frontal cortex through primary visual cortex (thin lines).

ratio on region size was stronger in the more severely affected cases with large contrasts between hypometabolic association areas and relatively normal denominator regions.

DISCUSSION

Use of a ratio instead of regional metabolic rates reduces variability because several factors that influence metabolism in all regions in the same direction tend to cancel out. This is completely the case for plasma glucose levels and the lumped constant, since they have a proportional effect on all regions. The influence of the physiological variation of global metabolism also is reduced (*18,19*). Influence of factors like variation of rate constants, scanner resolution and ROI size is more complex.

According to the operational equation (*10*), fixed rate constants are used to estimate the proportion of unmetabolized deoxyglucose contributing to total measured activity. The distribution volume of the compartment of unmetabolized tracer can be approximated by $K_1/(k_2 + k_3)$. Thus, an increase of K_1 or a decrease of k_2 or k_3 increases that estimate and reduces the calculated metabolic rate, as demonstrated in the simulation results. This effect is not proportional but essentially additive and therefore affects regions with low activity more than regions with high activity. It cancels out only if metabolic rates in the numerator and denominator of the ratio are similar, as is the case for normals, but not for severely affected patients. Thus, the ratio is still sensitive to rate constant variation in patients, but less sensitive than metabolic rates.

There is ample evidence that dephosphorylation of FDG in vivo is slow and may be neglected for measurement times of up to approximately 45 min (*20,21*). That was done in the centers in Milan and Cologne. In the center in Liège, measurement times were longer because of the necessity to use multiple bed positions to cover the entire brain and a non-zero k_4 was used appropriately. As shown in the simulation results, its influence on the ratio at earlier measurement times, as used in the centers in Milan and Cologne, would be very small (<1%).

Use of raw activity data instead of MRGlu could also be a potential alternative to avoid problems introduced by different rate constants and would have the advantage not to require blood sampling. Because of continuing tracer accumulation, use of raw activity-distribution instead of metabolic images is possible only if all relevant brain structures can be scanned at once. That requires a scanner with an axial field of view of at least 80 mm not available in all centers involved in the present study. Ratios derived from activity data would probably depend on measurement time and, because subtraction of unmetabolized tracer activity makes a larger difference in areas with low activity, would be higher in patients than those derived from MRGlu data.

Region size influenced the ratio more severely in patients than in normals. This is mainly due to high contrast between the relatively small, metabolically active putamen, primary visual and sensorimotor cortex regions and surrounding structures, whereas quantitation in the hypometabolic areas with reduced gray-to-white matter contrast is less sensitive to region size. Thus, in patients, numerator and denominator of the ratio are affected in a different way, whereas in normals, gray-to-white matter contrast is similar in all regions. The largest difference of average region size in our study was 21% (smaller in the center in Milan than in Cologne), resulting in an estimated ratio change of only 2.1%. The effect of region size and

TABLE 4
Areas Under the ROC Curves (Percent of Total Area) for Ratios Derived from Single Regions

Denominator regions	Numerator regions			
	Left temporoparietal	Right temporoparietal	Left frontal	Right frontal
Primary sensorimotor cortex	90.1	93.3	81.4	80.1
Primary visual cortex	88.6	89.7	79.0	75.7
Putamen	86.6	86.2	84.3	78.2
Cerebellum	95.7	93.9	87.1	86.1

spatial resolution was also studied (mainly in normals) by Grady et al. (*22*). Although they found 30%–120% higher metabolic rates in gray matter regions with a high-resolution scanner and small regions than with a low-resolution scanner and large regions, variation of ratios (region to average gray matter) was only ±5%. Effects of high spatial resolution and small region size together with the skewness of age distribution towards presenile dementia (*17*) most likely explain that the lowest ratios were recorded in the center in Milan. In spite of lower resolution and similar region size, the lower mean ratio value in patients in the center in Liège compared to those at the center in Cologne may be explained by the effect of the set of rate constants used there, that reduced average patient ratios by 7.7% in the simulation study.

To increase robustness, the ratio used in the present study was based on more regions than suggested by other authors, e.g., parietal cortex-to-striatum and thalamus (*7*), frontal or parietal cortex-to-primary sensorimotor cortex (*23*), or parieto-temporal-to-occipital cortex (*24*). Its construction reflects the typical metabolic alterations of AD. With a minor modification (exclusion of brainstem regions and omission of the adaptation of K_1 and k_3 to measured activity) it was taken from a previous study (*14*). The ROC curves (Fig. 4 and Table 4) demonstrate that its diagnostic accuracy is superior to most ratios derived from single regions and that there is no loss of sensitivity by averaging over all typically affected regions. It has been demonstrated in previous studies that the composite ratio can also discriminate between AD and dementia due to other conditions (*14,25*). Another advantage is that normal ratio values are close to unity, thus minimizing its sensitivity to variation of rate constants (with their predominantly additive shift effects on numerator and denominator), particularly in cases of early disease.

The increase of the ratio with patient age was already noted in an earlier study (*17*) and was reproduced here. It corresponds with other reports (*26,27*) that show contrast between temporoparietal association cortex and other brain areas is more pronounced in presenile than in senile dementia. The absence of age dependence of the ratio in normals facilitates its use.

The present study demonstrates that the ratio provides a solid basis to perform multicenter studies with FDG PET in AD, even if scanner resolution and some other technical details vary among laboratories. Simulation studies indicated that it is desirable to use the same set of rate constants and same region size in all centers. Although that was not achieved in the present study, results in the three centers were closely comparable. Residual differences of the ratio were not statistically significant, whereas there was a clear and consistent difference between patients and normals resulting in a high diagnostic accuracy.

ACKNOWLEDGMENTS

The authors thank S. Bressi, G. Striano, S. Todde, M. Matarrese, V. Bettinardi, M.C. Gilardi, J. Kessler, R. Mielke, M. Grond, J. Rudolf, K. Wienhard, U. Pietrzyk, R. Wagner and B. Bauer. This research was carried out within the framework of the European Community Medical and Health Research Program on PET Investigation of Cellular Regeneration and Degeneration.

REFERENCES

1. Benson DF, Kuhl DE, Hawkins RA, Phelps ME, Cummings JL, Tsai SY. The fluorodeoxyglucose ^{18}F scan in Alzheimer's disease and multi-infarct dementia. *Arch Neurol* 1983;40:711–714.
2. Friedland RP, Budinger TF, Ganz E, et al. Regional cerebral metabolic alterations in dementia of the Alzheimer type: positron emission tomography with (^{18}F) fluorodeoxyglucose. *J Comput Assist Tomogr* 1983;7:590–598.
3. Foster NL, Chase TN, Fedio P, Patronas NJ, Brooks RA, DiChiro G. Alzheimer's disease: focal cortical changes shown by positron emission tomography. *Neurology* 1983;33:961–965.
4. McGeer PL, Kamo H, Harrop R, et al. Positron emission tomography in patients with clinically diagnosed Alzheimer's disease. *Can Med Assoc J* 1986;134:597–607.
5. Duara R, Grady C, Haxby J, et al. Positron emission tomography in Alzheimer's disease. *Neurology* 1986;36:879–887.
6. Szelies B, Herholz K, Pawlik G, Beil C, Wienhard K, Heiss W-D. Zerebraler glukosestoffwechsel bei präseniler demenz vom Alzheimer-typ—verlaufskontrolle unter therapie mit muskarinergem cholinagonisten. *Fortschr Neurol Psychiatr* 1986;54:364–373.
7. Kuhl DE, Small GW, Riege WH, et al. Cerebral metabolic patterns before the diagnosis of probable Alzheimer's disease [Abstract]. *J Cereb Blood Flow Metab* 1987;7(suppl. 1):S406.
8. McKhann G, Drachman D, Folstein MF, Katzman R, Price D, Stadlan EM. Clinical diagnosis of Alzheimer's disease. *Neurology* 1984;34:939–944.
9. Folstein MF, Folstein SE, McHugh PR. Mini-mental state. *J Psychiatr Res* 1975;12:189–198.
10. Sokoloff L, Reivich M, Kennedy C, et al. The ^{14}C-deoxyglucose method for the measurement of local cerebral glucose utilization: theory, procedure and normal values in the conscious and anesthetized albino rat. *J Neurochem* 1977;28:897–916.
11. Huang S-C, Phelps ME, Hoffman EJ, Sideris K, Selin CJ, Kuhl DE. Noninvasive determination of local cerebral metabolic rate of glucose in man. *Am J Physiol* 1980;238:E69–E82.
12. Heiss W-D, Pawlik G, Herholz K, Wagner R, Göldner H, Wienhard K. Regional kinetic constants and cerebral metabolic rate for glucose in normal human volunteers determined by dynamic positron emission tomography of [^{18}F]-2-fluoro-2-deoxy-D-glucose. *J Cereb Blood Flow Metab* 1984;4:212–223.
13. Reivich M, Alavi A, Wolf A, et al. Glucose metabolic rate kinetic model parameter determination in humans: the lumped constant and rate constants for [^{18}F]fluorodeoxyglucose and [^{11}C]deoxyglucose. *J Cereb Blood Flow Metab* 1985;5:179–192.
14. Herholz K, Adams R, Kessler J, Szelies B, Grond M, Heiss WD. Criteria for the diagnosis of Alzheimer's disease with positron emission tomography. *Dementia* 1990;1:156–164.
15. Hanley JA, McNeil BJ. A method of comparing areas under receiver operating characteristic curves derived from the same cases. *Radiology* 1983; 148:839–843.
16. Herholz K, Pawlik G, Wienhard K, Heiss W-D. Computer assisted mapping in quantitative analysis of cerebral positron emission tomograms. *Comput Assist Tomogr* 1985;9:154–161.
17. Mielke R, Herholz K, Grond M, Kessler J, Heiss WD. Differences of regional cerebral glucose metabolism between presenile and senile dementia of Alzheimer type. *Neurobiol of Aging* 1992;13:93–98.
18. Camargo EE, Szabo Z, Links JM, Sostre S, Dannals RF, Wagner HN. The influence of biological and technical factors on the variability of global and regional brain metabolism of 2-[F-18]fluoro-2-deoxy-D-glucose. *J Cereb Blood Flow Metab* 1992;12:281–290.
19. Bartlett EJ, Brodie JD, Wolf AP, Christman DR, Laska E, Meissner M. Reproducibility of cerebral glucose metabolic measurements in resting human subjects. *J Cereb Blood Flow Metab* 1988;8:502–512.
20. Nelson T, Lucignani G, Sokoloff L. Measurement of brain deoxyglucose metabolism by NMR. *Science* 1986;232:776–777.
21. Kotyk JJ, Rust RS, Ackerman JJH, Deuel RK. Simultaneous in vivo monitoring of cerebral deoxyglucose and deoxyglucose-6-phosphate by C-13(H-1) nuclear magnetic-resonance spectroscopy. *J Neurochem* 1989; 53:1620–1628.
22. Grady CL, Berg G, Carson RE, Daube-Witherspoon ME, Friedland RP,

Rapoport SI. Quantitative comparison of cerebral glucose metabolic rates from two positron emission tomographs. *J Nucl Med* 1989;30:1386–1392.
23. McNamara D, Horwitz B, Grady CL, Rapoport SI. Topographical analysis of glucose metabolism, as measured with positron emission tomography, in dementia of the Alzheimer type: use of linear histograms. *Int J Neurosci* 1987;36:89–97.
24. Duara R, Barker W, Pascal S, Chang JY, Apicella A, Loewenstein D. The sensitivity and specificity of PET in aging and dementia. *J Cereb Blood Flow Metab* 1989;9(suppl. 1):567.
25. Mielke R, Herholz K, Grond M, Kessler J, Heiss W-D. Severity of vascular dementia is related to volume of metabolically impaired tissue. *Arch Neurol* 1992;49:909–913.
26. Grady CL, Haxby JV, Horwitz B, Berg G, Rapoport S. Neuropsychological and cerebral metabolic function in early versus late onset dementia of the Alzheimer type. *Neuropsychologia* 1987;25:807–816.
27. Small GW, Kuhl D, Riege WH, et al. Cerebral glucose metabolic patterns in Alzheimer's disease. Effect of gender and age at dementia onset. *Arch Gen Psych* 1989;46:527–532.